HHS Public Access

Author manuscript

Biochim Biophys Acta Mol Cell Res. Author manuscript; available in PMC 2025 January 01.

Published in final edited form as:

Biochim Biophys Acta Mol Cell Res. 2024 January ; 1871(1): 119590. doi:10.1016/j.bbamcr.2023.119590.

Protein Tyrosine Phosphatase 1B is a Regulator of Alpha-Actinin4 in the Glomerular Podocyte

Ming-Fo Hsu[1,†], **Yoshihiro Ito**[1,†,#], **Jai Prakash Singh**[2], **Shu-Fang Hsu**[2], **Alan Wells**[3], **Kuang-Yu Jen**[4], **Tzu-Ching Meng**[2], **Fawaz G. Haj**[1,5,6,*]

[1]Department of Nutrition, University of California Davis, Davis, CA, USA

[2]Institute of Biological Chemistry, Academia Sinica, Nankang, Taipei, Taiwan

[3]Department of Pathology, University of Pittsburgh Medical Center, Pittsburgh, PA, USA

[4]Department of Pathology and Laboratory Medicine, University of California Davis, Sacramento, CA, USA

[5]Comprehensive Cancer Center, University of California Davis, Sacramento, CA, USA

[6]Division of Endocrinology, Diabetes, and Metabolism, Department of Internal Medicine, University of California Davis, Sacramento, CA, USA

Abstract

Glomerular podocytes are instrumental for the barrier function of the kidney, and podocyte injury contributes to proteinuria and the deterioration of renal function. Protein tyrosine phosphatase 1B (PTP1B) is an established metabolic regulator, and the inactivation of this phosphatase mitigates podocyte injury. However, there is a paucity of data regarding the substrates that mediate PTP1B actions in podocytes. This study aims to uncover novel substrates of PTP1B in podocytes and validate a leading candidate. To this end, using substrate-trapping and mass spectroscopy, we identified putative substrates of this phosphatase and investigated the actin cross-linking cytoskeletal protein alpha-actinin4. PTP1B and alpha-actinin4 co-localized in murine and human glomeruli and transiently transfected E11 podocyte cells. Additionally, podocyte PTP1B deficiency *in vivo* and culture was associated with elevated tyrosine phosphorylation of alpha-actinin4. Conversely, reconstitution of the knockdown cells with PTP1B attenuated alpha-actinin4 tyrosine phosphorylation. We demonstrated co-association between alpha-actinin4 and the PTP1B substrate-trapping mutant, which was enhanced upon insulin stimulation and disrupted by vanadate, consistent with an enzyme-substrate interaction. Moreover, we identified alpha-actinin4 tandem tyrosine residues 486/487 as mediators of its interaction with PTP1B. Furthermore, knockdown studies in E11 cells suggest that PTP1B and alpha-actinin4 are modulators of podocyte motility. These observations indicate that PTP1B and alpha-actinin4 are

[*]**Corresponding author:** Fawaz G. Haj, The University of California Davis, Department of Nutrition, 3135 Meyer Hall, Davis, CA 95616, USA, fghaj@ucdavis.edu.

[#]**Current address:** Department of Endocrinology and Diabetes, Nagoya University Graduate School of Medicine, Nagoya, Japan

[†]**Equal contribution and first authorship:** These authors contributed equally to this work and shared the first authorship

Author contributions: **Y.I.**, **M-F.H.**, **T-C.M.**, and **F.G.H.** designed research; **Y.I.**, **M-F.H.**, **J.P.S.**, and **S-F.H.**, performed research; **Y.I.**, **M-F.H.**, **J.P.S.**, **S-F.H.**, **T-C.M.**, and **F.G.H.** analyzed data; **A.W.** and **K-Y.J.** provided materials; and all authors wrote, reviewed, and revised the manuscript.

Conflict of Interest: The authors declare no competing financial interests.

likely interacting partners in a signaling node that modulates podocyte function. Targeting PTP1B and plausibly this one of its substrates may represent a new therapeutic approach for podocyte injury that warrants additional investigation.

Keywords

protein tyrosine phosphatase 1B; alpha-actinin4; podocytes; insulin signaling; tyrosine phosphorylation; cell motility

Introduction

The glomerulus is the kidney's core filtration unit, and glomerular dysfunction contributes to proteinuria and kidney disease. Podocytes are specialized cells crucial for glomerular filtration barrier function and structural integrity [1, 2]. Podocytes exhibit unique morphology where interdigitating foot processes generate a specific intercellular junction termed the slit diaphragm [3, 4]. Many components of the slit diaphragm are anchored to the cytoskeleton, and podocyte injury disrupts the cytoskeleton leading to loss of filtration barrier integrity (reviewed in ref. [5]). In humans, several mutations in podocyte-specific genes result in congenital or familial proteinuria and often lead to end-stage renal failure [6]. Therefore, deciphering the molecular mechanisms that modulate podocyte architecture and injury is desirable and of translational relevance.

Alpha-actinins (ACTNs) are a conserved family of actin cross-linking cytoskeletal proteins implicated in myriad cellular functions, including cytoskeletal remodeling [7–9]. Alpha-actinins contain three distinct modules: an N-terminal actin-binding domain, four spectrin-like repeats, and a C-terminal calmodulin-binding domain, with the spectrin-like repeats forming antiparallel homodimers that cross-link actin filaments [10, 11]. In humans, four alpha-actinins are described with actinin1 and actinin4 ubiquitously expressed [12]. In particular, alpha-actinin4 is highly expressed in podocytes and significantly contributes to podocyte architecture [13, 14]. Notably, mutations in the *ACTN4* gene are responsible for a highly penetrant, autosomal dominant form of familial focal segmental glomerulosclerosis (FSGS) in humans [15–17]. On biopsy, this disorder exhibits the typical light microscopy and ultrastructural changes, namely focal and segmental glomerular scarring and diffuse podocyte foot process effacement, with the additional distinctive finding of electron-dense aggregates within the podocytes [18]. Transgenic mice overexpressing the alpha-actinin4 K256E mutant (analogous to the FSGS-causing mutation in humans) exhibit spontaneous albuminuria and podocyte foot enfacement (reviewed in ref. [14]). Additionally, alpha-actinin4 influences podocyte adhesion and regulates the actin cytoskeleton interaction with the plasma membrane [19, 20]. Indeed, alpha-actinin4 mutations disrupt the cytoskeleton and compromise the podocyte's ability to handle the demands of the glomerular milieu [21, 22]. Moreover, post-translational modifications to alpha-actinin4, such as tyrosine phosphorylation downstream from receptor protein tyrosine kinases (RTKs) [23, 24], is critical for stress fiber establishment, maintenance, and focal adhesion maturation [25]. As tyrosine phosphorylation is readily reversible, we expect this cellular function to

be modulated bidirectionally, but the tyrosine phosphatase(s) that regulate alpha-actinin4 phosphorylation in podocytes is not currently known.

The prototypical protein tyrosine phosphatase 1B (PTP1B; encoded by *Ptpn1*) is a ubiquitously expressed non-receptor phosphatase that is anchored on the cytoplasmic surface of the endoplasmic reticulum (ER) [26, 27]. PTP1B regulates many aspects of signaling by selectively engaging diverse substrates and pathways (reviewed in refs. [28, 29]). Notably, PTP1B is a recognized regulator of metabolism *in vivo* and a therapeutic target for obesity and type 2 diabetes (reviewed in refs. [30, 31]). Several lines of evidence implicate podocyte PTP1B in renal function and suggest that pharmacological inhibition of this phosphatase may have therapeutic potential for proteinuric diseases. Whole-body PTP1B disruption in mice attenuates complement-mediated glomerular injury [32]. Additionally, podocyte-specific PTP1B disruption mitigates proteinuria induced by adriamycin and lipopolysaccharide [33] and ameliorates hyperglycemia-induced renal injury [34]. Moreover, nephrin, a key component for filtration barrier integrity, is a PTP1B substrate [35]. Furthermore, the insulin receptor (IR), an RTK, is a *bona fide* substrate of PTP1B and a significant regulator of podocyte function *in vivo* [36]. Indeed, PTP1B antagonizes insulin signalin, at least in large part, by dephosphorylation of the critical tyrosine residues on IR [29]. However, these pathways do not fully account for PTP1B actions in podocytes. This study deployed biochemical, genetic, and cellular approaches to identify novel putative substrates of PTP1B in podocytes and validated a leading candidate, alpha-actinin4.

Materials and Methods

Reagents.

RPMI1640, Opti-MEM, penicillin/streptomycin, puromycin, hygromycin, fetal bovine serum (FBS), and trypsin were purchased from Invitrogen. The recombinant insulin solution (Humulin R, U-100) was from Eli Lilly and Company. Antibodies for phospho-tyrosine (4G10) and human PTP1B (hPTP1B, FG6) from EMD Millipore; phospho-tyrosine (PY99), PTP1B, green fluorescent protein (GFP), Synaptopodin, and Actin from Santa Cruz Biotechnology; alpha-actinin4 from Cell Signaling Technology; mouse PTP1B (mPTP1B) from R & D Systems. The HRP-conjugated secondary antibodies were purchased from Bio-Rad Laboratories. De-identified human kidney biopsies were provided by Dr. Jen (UC Davis Medical Center).

Cell culture.

We cultured the E11 murine kidney podocyte cells (Cell Lines Service) at 33°C in RPMI medium supplemented with 2mM L-glutamine and 10% FBS and induced to differentiate by culturing at 37°C for 14 days [37]. PTP1B knockdown (KD) was performed as previously described [38, 39]. PTP1B knockdown cells were reconstituted with wild-type human PTP1B (KD-WT) or the substrate-trapping human PTP1B D181A mutant (KD-D/A), and cell lines were generated by hygromycin (400μg/mL) selection as described [40]. Alpha-actinin4 silencing was achieved using ON-TARGET plus siRNAs-Mouse (GE Dharmacon, 10nM) with Hiperfect (Qiagen) according to manufacturer’s instruction. To express eGFP-

ACTN4 WT and $Y^{486/487}F$ for immunofluorescence staining, cells were co-transfected with ACTN4 siRNA (10nM, to decrease the endogenous alpha-actinin4) and 4μg plasmids of eGFP-ACTN4 constructs by Lipofectamine 3000 (Invitrogen) following the manufacturer's guidelines. Briefly, cells were seeded in 6cm culture plates at a density of 2.0×10^4 cells/cm^2 and cultured in antibiotic-free RPMI1640. Cells were incubated with transfection complexes for 6 hours in Opti-MEM. Media were changed 6 hours after transfection, and cells were used following an additional 42 hours of incubation under normal growth conditions. For insulin stimulation, knockdown and reconstituted podocytes were starved overnight in RPMI medium without FBS then incubated with 10nM insulin, and the cell lysates were collected at the times as indicated in the figures. For the scratch migration assay, E11 cells were serum starved overnight, and the wound was generated using a 200μL pipette tip. Cells were incubated in RPMI medium (10% FBS) for additional 48 hours. Images were acquired using Olympus BX51 microscope at 0, 24, and 48 hours. Cell migration was quantitated by the manual counting of the cells in the wound.

Biochemical analyses.

Frozen tissues were ground in liquid nitrogen and then lysed using radioimmunoprecipitation assay (RIPA) buffer (10mM Tris-HCl pH 7.4, 150mM NaCl, 0.1% sodium dodecyl sulfate, 1% Triton X-100, 1% sodium deoxycholate, 5mM EDTA, 20mM NaF, 2mM sodium orthovanadate, and protease inhibitors). For the substrate-trapping studies, we lysed the E11 cells in Nonidet P-40 buffer (10mM Tris-HCl pH 7.4, 150mM NaCl, 1% IGEPAL™ CA-630) with protease inhibitors (without sodium orthovanadate). Additionally, cell lysates prepared using RIPA buffer or including sodium orthovanadate (2mM) served as negative controls. Protein concentrations were determined by a bicinchoninic acid protein assay kit (BCA, Pierce Chemical), then resolved using SDS-PAGE and transferred to PVDF membranes. To do the immunoprecipitation (IP) and substrate-trapping experiments, total lysates with equal protein amounts were incubated with the primary antibodies, followed by the protein A/G magnetic beads (EMD Millipore). The immune complexes on protein A/G magnetic beads were washed and eluted. Immunoblotting was performed using the indicated primary antibodies. After incubation with secondary antibodies, the proteins were visualized using enhanced chemiluminescence (HyGLO; Denville Scientific). Immunoblotting images were further quantified by the FluorChem 9900 program (Alpha Innotech). For site-directed mutagenesis, cDNA of alpha-actinin4 tagged by eGFP at the C-terminus (eGFP-ACTN4 WT), 4/31 Y/F, and 265 Y/F mutants were provided by Dr. Wells (University of Pittsburgh) [23]. Additionally, mutation of alpha-actinin4 tyrosine 468/487 residues to phenylalanine was performed using a QuikChange Lightning site-directed mutagenesis kit (Agilent Technologies) following the manufacturer's instructions and confirmed by DNA sequence analysis.

LC-MS/MS mass spectrometry.

We differentiated the KD-D/A cells, starved them overnight, then stimulated with insulin as described before [34]. hPTP1B was immunoprecipitated from the cell lysates prepared with Nonidet P-40 or RIPA buffer. Proteins were resolved by SDS-PAGE, and the gel was stained using Instant Blue (Expedeon). The 60, 70, 80, 100, and 170 kDa bands from 10- and 20- minutes insulin stimulation were excised and subjected to in-gel trypsin digestion

for peptides release. Tryptic peptides were separated by an integrated reverse-phase chromatography system (Easy-nLC, Proxeon Biosystems) and then analyzed on a Linear Quadrupole ION Trap/Finnigan Polaris Q Mass Spectrometer (Thermo Fisher Scientific). The tandem mass spectra were converted by ReadW.exe program using a centroid mode, and peptide sequences were matched by X!Tandem algorithm against the mouse database from the International Protein Index. Also, we used Scaffold (Proteome Software) to validate MS/MS-based peptide and protein identifications as described [41].

Protein expression and purification.

PTP1B construct (residue: 1–321) containing an N-terminal His_6-tag (vector: pMCSG7) was transformed into *E.Coli* BL21 (DE3) strain. Cells were grown in Luria broth medium containing selective antibiotics at 37°C to an OD_{600} of ~0.6. Subsequently, 1mM Isopropyl β-D-1-thiogalactopyranoside (IPTG) was added to induce expression. Afterward, the temperature of the incubator was reduced to 18°C, and expression was continued overnight. Cells were harvested by centrifugation at 6000 RPM for 20 min using JLA 8.1 rotor in an Avanti J-26-XPI Centrifuge.

To purify the protein, harvested cells were dissolved in lysis buffer containing 50 mM Tris-HCl pH 7.4, 500mM NaCl, 5% Glycerol, and protease inhibitor cocktail tablet (EDTA free). Cells were lysed by TS-series cell disrupter (Constant System Ltd.). Lysates were centrifuged at 20000 RPM for 30 minutes at 4°C using JA 25.5 rotor in an Avanti J-26-XPI Centrifuge. Supernatants were collected and mixed with 5mL of Ni-NTA resins for ~2 hours at 4°C on a rotating shaker. Resins were washed with 100mL of wash buffer containing 50mM Tris-HCl pH 7.4, 500mM NaCl, 5% Glycerol, and 25mM Imidazole. Bound proteins from Ni-NTA resins were eluted by elution buffer consisting of 50 mM Tris-HCl pH 7.4, 500mM NaCl, 5% Glycerol, and 350mM Imidazole. Eluents from Ni-NTA resins were dialyzed overnight in the presence of TEV protease to remove N-terminal His-tag against 3L of dialysis buffer containing 50mM Tris-HCl pH 7.4, 500mM NaCl, 5% Glycerol, and 0.5 mM TCEP, at 4°C. After dialysis, reverse Ni-NTA purification was performed to separate the proteins without tag from the proteins containing a tag. The flowthrough of reverse Ni-NTA, containing proteins without tag, was applied to size exclusion chromatography (SEC) for further purification. For SEC, a HiLoad Superdex 200 16/600 column (GE Healthcare) was used. Before applying proteins, the column was equilibrated with a buffer consisting of 50mM Tris-HCl pH 7.4, 150mM NaCl, and 10mM DTT.

Peptide Synthesis.

All alpha-actinin4 derived mono-phospho-tyrosine peptides (ELDpYYDSHN and ELDYpYDSHN), and di-phospho-tyrosine peptide (ELDpYpYDSHN) were synthesized by the Peptide Synthesis Core Facility at the Institute of Biological Chemistry, Academia Sinica, Taiwan. After synthesis, the final purity of the peptides was determined to be ≥90% based on HPLC and mass spectrometry analysis.

Enzyme kinetic assay.

The rate of dephosphorylation of PTP1B (residue 1–321) against mono-phospho-tyrosine (ELDpYYDSHN or ELDYpYDSHN) and di-phospho-tyrosine (ELDpYpYDSHN) peptides

was monitored in the assay buffer containing 50mM Tris-HCl pH 7.4, 150mM NaCl, and 1mM DTT. Lyophilized powder of all synthetic peptides was dissolved in DMSO to generate a stock solution at 5mM. For the kinetic assay, the concentration of the enzyme (PTP1B) was fixed at 1nM while the substrate (phosphopeptides) concentrations varied from 2.5μM to 160μM in a total reaction volume of 200μL. The reaction mixture was incubated at 30°C for 30 min, then stopped by the addition of 30μL phosphate reagent (phosphate colorimetric assay kit; Bio Vision) following the manufacturer's instructions. Data were normalized and fitted using a nonlinear curve. The kinetics parameters (K_M and k_{cat}) were calculated from the Michaelis-Menten equation using Graph Pad Prism 9.0. All data points in the enzyme kinetics experiment were measured in triplicate, and the experiments were repeated three times independently.

Mouse studies.

PTP1B floxed (*Ptpn1*$^{fl/fl}$) mice [42] were bred to podocin-Cre transgenic mice (Jackson Laboratories) to generate mice with podocyte-specific PTP1B disruption as described [32–34]. All mice studied were age-matched and maintained on a 12-hour light-dark cycle in a temperature-controlled facility, with free access to water and standard laboratory chow (Purina lab chow, # 5001). For the high-fat diet (HFD) studies, 8 weeks old male mice were fed HFD (60% kcal from fat, # D12492, Research Diets) for 25 weeks. For the streptozotocin (STZ) challenge, male mice (8–12 weeks old) were injected intraperitoneally (IP) with STZ (Amresco) at 160μg/g body weight and sacrificed at 13 weeks post-injection. For insulin stimulation, overnight fasted male mice were intraperitoneal injected with insulin (10mU/g body weight), and animals were sacrificed after 10 min. All mouse studies were approved by the Institutional Animal Care and Use Committee at the University of California, Davis.

Histology and immunofluorescence.

Kidneys from mice fed standard laboratory chow, a HFD, or treated with STZ were fixed in 4% paraformaldehyde/PBS and embedded in paraffin. Human and mouse kidney sections were deparaffinized/rehydrated in xylene/graded ethanol. For E11 cell staining, the cultured on coverslips were fixed with 100% ice-cold methanol for 10 minutes. Samples were blocked with 3% BSA/PBS for 1 hour at room temperature and incubated with primary antibodies for alpha-actinin4, hPTP1B, PTP1B, GFP, and Synaptopodin at 4°C overnight. Then appropriate Alexa Fluor-conjugated secondary antibodies (Thermo Fisher Scientific; 488-anti-rabbit, 555-anti-goat, 555-anti-mouse, 647-anti-mouse) were incubated at room temperature for 1 hour. Finally, samples were mounted with Mowiol (Sigma) solution and examined using Olympus FV1000 confocal microscope.

Statistical analyses.

Data were expressed as means + standard error of the mean (SEM). Statistical analyses were performed by the SPSS program (IBM) to compare differences between groups using one-way ANOVA with the Tukey post hoc test. Differences were considered significant at $p \leq 0.05$.

Results

Identification of putative substrates of PTP1B in podocytes.

Comprehensive and unbiased determination of PTP1B substrates is instrumental for deciphering the role of this phosphatase in podocytes. To this end, we used the substrate-trapping approach that entails mutating the catalytic acid (Asp181 in PTP1B, rendering a stable interaction of the mutant enzyme and its substrate) that is conserved in all members of the PTP family [43]. Briefly, we generated E11 podocyte cell lines by reconstituting the PTP1B knockdown (KD) cells [34] with the shRNA-resistant human (h) PTP1B wild-type (KD-WT) and substrate-trapping mutant (D181A; KD-D/A) (Figure 1A). Immunoblots demonstrated PTP1B deficiency in the knockdown cells and expression in the reconstituted podocytes (Figure 1B). Additionally, cells with PTP1B knockdown did not exhibit an apparent compensatory increase in the expression of the closely-related T-cell protein-tyrosine phosphatase [44]. To identify putative PTP1B substrates, we immunoprecipitated hPTP1B from the 14 days-differentiated KD-D/A cells under basal and insulin stimulation, resolved using SDS-PAGE, then immunoblotted for phospho-tyrosine. Upon insulin stimulation, we detected hyper-phosphorylated proteins in NP40-lysed podocytes (at about 60, 70, 80, 110, and 170 kDa) that likely corresponded to the “trapped” putative PTP1B substrates (Figure 1C). The insulin-induced tyrosine phosphorylation was diminished using RIPA, with the stringent lysis conditions likely disrupting the co-association of PTP1B D/A and its targets. In a parallel experiment, we stained a comparable gel with Instant Blue, excised the bands corresponding to the hyper-phosphorylated proteins, and subjected them to mass spectrometry as detailed in the methods. We identified several novel putative substrates of PTP1B in addition to others that were previously reported, such as cortactin [45] (Figure 1D). We employed several criteria to select a candidate for validation, including the total spectrum counted by the mass spectrometer, the target’s tyrosine residue(s) and their reported impact on function, sub-cellular localization, and the proposed role in podocytes. Accordingly, the actin cross-linking cytoskeletal protein alpha-actinin4 emerged as one of the leading candidates for further analyses.

Alpha-actinin4 interacts with PTP1B.

To investigate if alpha-actinin4 is a substrate of PTP1B in podocytes, we initially examined the localization and association of these proteins and then determined the impact of PTP1B deficiency on alpha-actinin4 tyrosine phosphorylation. Accordingly, we evaluated the expression of PTP1B and alpha-actinin4 in human and murine glomeruli using immunofluorescence. Confocal images of kidney sections co-immunostained for endogenous alpha-actinin4 and PTP1B demonstrated partial co-localization in human and murine glomeruli (Figure 2A, B). Additionally, PTP1B immunoreactivity was likely elevated under STZ- and HFD-induced hyperglycemia (Figure 2B). Having demonstrated co-localization in the glomeruli, next, we monitored the effects of PTP1B deficiency in E11 cells and *in vivo* on alpha-actinin4 tyrosine phosphorylation. Using E11 cells with the knockdown and reconstituted expression of PTP1B, we immunoprecipitated alpha-actinin4 under basal and insulin stimulation and then immunoblotted for phospho-tyrosine. Indeed, alpha-actinin4 tyrosine phosphorylation was elevated in the cells with PTP1B knockdown and D/A reconstitution (Figure 3A). Moreover, we evaluated alpha-actinin4 phosphorylation

in control (Ctrl; *Ptpn1*$^{fl/fl}$) mice and those with podocyte-specific PTP1B disruption (pod-PTP1B KO; *Ptpn1*$^{fl/fl}$ Pod-cre^{+}) under basal and insulin stimulation. We fasted mice overnight to lower their insulin to the basal level, then injected saline or insulin and sacrificed them after 10 minutes. Subsequently, we immunoprecipitated alpha-actinin4 from the kidney lysates and immunoblotted for phospho-tyrosine. Notably, insulin stimulation elevated alpha-actinin4 tyrosine phosphorylation in both genotypes but to a significantly greater extent in mice with PTP1B disruption (Figure 3B). Next, we examined the interaction of these proteins using the substrate-trapping approach. We immunoprecipitated hPTP1B from the KD-D/A cells under basal and insulin stimulation and then immunoblotted for alpha-actinin4. We detected minimal co-association of alpha-actinin4 and PTP1B D/A at the basal state, but that was robustly enhanced upon insulin stimulation (10 and 20 minutes) (Figure 3C). Significantly, treatment with vanadate abrogated the co-association consistent with an enzyme-substrate interaction that is mediated by the phosphatase's catalytically active site. Taken together, the co-localization of these proteins, the elevated tyrosine phosphorylation of alpha-actinin4 upon PTP1B deficiency, and the substrate-trapping observations are in keeping with alpha-actinin4 being a substrate for this phosphatase.

Alpha-actinin4 tandem tyrosine-phosphorylated motif mediates the interaction with PTP1B.

Having demonstrated the co-association of alpha-actinin4 and PTP1B, we aimed to identify the motif(s) in the former that mediate the interaction. Alpha-actinin4 contains twenty-five tyrosine residues, including tandem residues 486–487 (D-Y-Y-D) that are evolutionarily conserved among several species (Figure 4A). Compelling evidence demonstrates a higher affinity of PTP1B for tandem pTyr-containing peptides than mono-pTyr derivatives and highlights the sequence E/D-pY-pY-R/K as important for substrate recognition [46]. Using a tyrosine (Y) to phenylalanine (F) mutagenesis approach, we determined the effect of mutating key alpha-actinin4 tyrosine residues (Y$^{4/31}$F, and Y^{265}F) [23, 47] and the tandem residues (Y$^{486/487}$F) on its interaction with PTP1B. To this end, we transfected KD-D/A cells with eGFP-alpha-actinin4 wild-type (WT) and mutants (Y$^{4/31}$F, Y^{265}F, and Y$^{486/487}$F), stimulated with insulin, then immunoprecipitated hPTP1B and immunoblotted for GFP. Insulin stimulation induced a robust co-association between PTP1B D/A and alpha-actinin4 WT, Y$^{4/31}$F, and Y^{265}F, but not Y$^{486/487}$F (Figure 4B). Additionally, we used confocal imaging to monitor the co-localization. Briefly, we co-transfected KD-D/A cells with eGFP-alpha-actinin4 WT and Y$^{486/487}$F, then assessed localization under basal and insulin stimulation. In keeping with observations from the biochemical studies, insulin induced the co-localization of PTP1B D/A and alpha-actinin4 WT, but that was diminished with the Y486/487F mutant (Figure 4C). Furthermore, to substantiate the direct interaction of alpha-actinin4 with PTP1B through the tandem tyrosine-phosphorylated motif, we performed an enzyme kinetic assay *in vitro*. The mono-phospho-tyrosine peptide (ELDpYYDSHN or ELDYpYDSHN) and di-phospho-tyrosine peptide (ELDpYpYDSHN) were incubated with the purified PTP1B (residues 1–321) as detailed in the methods. As expected, PTP1B dephosphorylated all phospho-tyrosine peptides following Michaelis-Menten kinetics (Figure 4D), suggesting an enzyme-substrate interaction. The kinetic parameters deduced by fitting the Michaelis-Menten equation showed nearly similar k_{cat} for all three peptides. However, the K_M for di-phospho-tyrosine peptide was ~3-fold lower

than mono-phospho-tyrosine peptides, suggesting a higher affinity of PTP1B towards the tandem tyrosine-phosphorylated alpha-actinin4 (Figure 4E). Similarly, the k_{cat}/K_M for the di-phospho-tyrosine peptide was found ~3 fold higher than the mono-phospho-tyrosine peptides (Figure 4E). These results highlight that the di-phospho-tyrosine peptide of alpha-actinin4 is a preferred target of PTP1B. Altogether, these findings demonstrate that alpha-actinin4 tandem tyrosine residues 486/487 contribute to the interaction with PTP1B.

Alpha-actinin4 and PTP1B modulate podocyte motility.

To delineate the potential contributions of alpha-actinin4 and PTP1B to podocyte functions, we determined the impact of their silencing on podocyte motility. Briefly, we performed siRNA-mediated knockdown of alpha-actinin4 in cells with PTP1B knockdown and reconstitution and then monitored alterations in motility. Of note, cells with alpha-actinin4 knockdown did not exhibit altered expression of the related alpha-actinin1 (data not shown). We evaluated the effects of knockdown on podocyte motility using the wound healing assay as detailed in the methods. We observed a significantly lower number of PTP1B-deficient cells in the wound (at 24 and 48 hours) compared with the PTP1B-reconstituted cells suggesting that the deficiency of this phosphatase diminished podocyte motility (Figure 5A). On the other hand, alpha-actinin4 knockdown in the PTP1B reconstituted cells was associated with a higher number of cells in the wound (at 24 and 48 hours) but did not significantly impact cells with PTP1B deficiency. These observations suggest that PTP1B and alpha-actinin4 are components of a signaling mode that likely affects podocyte motility (Figure 5B).

Discussion

The present study investigates the molecular underpinnings of PTP1B action in podocytes and suggests that this phosphatase may engage multiple targets to modulate podocyte function. Indeed, the substrate-trapping studies identified several putative mediators of PTP1B action. Herein, we validated one of the leading candidates, the actin cross-linking protein alpha-actinin4, and reported that PTP1B and alpha-actinin4 are likely interacting partners in a signaling node that affects podocyte function. Targeting PTP1B and plausibly this one of its substrates may represent a new approach for alleviating podocyte injury.

Multiple observations are in keeping with alpha-actinin4 being a likely substrate of PTP1B in podocytes. **1**) Substrate trapping and mass spectroscopy identified alpha-actinin4 as a leading putative PTP1B target in podocytes (Figure 1). Compelling evidence establishes the utility of the substrate trapping approach for identifying PTP1B substrates [39, 43, 45, 48–51]. Of note, cortactin, a reported substrate of this phosphatase [45], was identified in the current screen, further supporting the validity of this approach. **2**) Endogenous PTP1B and alpha-actinin4 partially co-localized in the human and murine glomeruli (Figure 2). Additionally, insulin enhanced the co-association and co-localization of exogenous PTP1B D/A and alpha-actinin4 in E11 cells, concomitant with increased tyrosine phosphorylation of the latter (Figures 3C and 4C and data not shown). The dynamic regulation of PTP1B and alpha-actin4 expression in the glomeruli remains to be established. However, PTP1B is upregulated in murine models under hyperglycemia [34] and podocyte injury [33], whereas

alpha-actinin4 is downregulated in patients with diabetic nephropathy [52]. 3) Podocyte PTP1B deficiency *in vivo* and culture was associated with elevated tyrosine phosphorylation of alpha-actinin4 (Figure 3A, B). Significantly, reconstitution of the knockdown cells with hPTP1B WT "rescued" these effects and attenuated alpha-actinin4 tyrosine phosphorylation. The mouse and human PTP1B are highly homologous, and human PTP1B can rescue mouse PTP1B deficiency [40, 53]. The current observations are in keeping with the direct regulation of alpha-actinin4 tyrosine phosphorylation by PTP1B. However, indirect regulation cannot be ruled out, for example, through the PTP1B substrates EGFR and Src [54], which modulate alpha-actinin4 phosphorylation [23]. **4**) Biochemical studies using the substrate-trapping mutant PTP1B D/A demonstrated co-association with alpha actin4 that was enhanced upon insulin stimulation (Figure 3C). However, we cannot exclude indirect association with both molecules being part of a joint multi-molecular complex, where another component is a PTP1B substrate. Of note, vanadate treatment that oxidizes the catalytic cysteine of the phosphatase [55] disrupted the co-association in line with an enzyme-substrate interaction mediated by the phosphatase's active site. Altogether, these findings are in keeping with alpha-actinin4 being a substrate of PTP1B, and a pressing challenge is to delineate the relevant contribution(s) of this interaction to podocytes.

Alpha-actinin4 tandem tyrosine 486/487 residues mediate the interaction with PTP1B, as evidenced by mutagenesis and cellular and biochemical analyses (Figure 4). However, other alpha-actinin4 tyrosine residue(s) may directly or indirectly contribute to the interaction with PTP1B. For instance, alpha-actinin4 phosphorylation on Tyr^4 serves as a switch that controls the accessibility of Tyr^{31} to its modifying kinase [56]. Moreover, PTP1B may target other members of the alpha-actinin family that contain the tandem pTyr target sequence, which is present in the non-muscle alpha-actinin (1 and 4) but not the muscle alpha-actinin (2 and 3). Indeed, in fibroblasts, PTP1B dephosphorylates alpha-actinin1 and regulates cell migration [57]. We also cannot ensure the interaction is with dually phosphorylated protein since replacing any single tyrosine with phenylalanine might shift the phosphorylation to the other tyrosine. Still and significantly, the current observations are consistent with PTP1B displaying a preference for select substrates containing E/D-pY-pY-R/K [46], with this motif helping to predict the PTP1B substrates Janus kinase2 and tyrosine kinase2 [58]. Additionally, the IR tandem tyrosine 1162/1163 residues mediate the interaction with PTP1B [46]. It is important to note that the dephosphorylation kinetic constants of PTP1B and the bisphosphorylated alpha-actinin4 peptide (K_M: 7.81 μM, k_{cat}: 16.98 s^{-1}, $k_{cat}/K_M \times 10^{-3}$: 2174.13 M^{-1} S^{-1}) (Figure. 3E) are comparable to those of PTP1B and the IR peptide (K_M: 7.5 μM, k_{cat}: 11.3 s^{-1}, $k_{cat}/K_M \times 10^{-3}$: 1514 M^{-1} S^{-1}) [46].

The interaction of PTP1B and alpha-actinin4 presents a potential mechanism that may affect podocyte function. However, these molecules likely engage other partners and participate in multiple tiers of signal regulation. The IR is a *bona fide* PTP1B substrate and a significant regulator of podocyte function *in vivo* [36]. Moreover, nephrin is an established PTP1B substrate that may mediate the actions of this phosphatase in some kidney disease models [33, 59] but not in others [32]. Furthermore, we uncovered other putative substrates of PTP1B in podocytes that require validation (Figure 1D and data not shown). Other PTP(s) may also target alpha-actinin4 and regulate its phosphorylation in podocytes. Indeed, there

is a precedent for multiple PTPs regulating essential podocyte proteins. For instance, the phosphorylation of nephrin is modulated by PTP1B [35] and the Src homology 2 domain-containing phosphatases Shp1 [60] and Shp2 [61, 62]. Moreover, PTP1B localization on the ER may impose some topological restrictions on the interactions of this enzyme with its substrates [27, 63]. Accordingly, PTP1B may engage alpha-actinin4 in the cytosol but not in the nucleus, where the latter is implicated in transcriptional activation [64–66]. Thus, different PTP(s) may engage alpha-actinin4 at various subcellular locations and orchestrate the dynamic regulation of this crucial molecule in podocytes.

PTP1B and alpha-actinin4 are components of a signaling node that impacts motility in podocytes. Significantly, PTP1B deficiency was associated with diminished podocyte motility, while alpha-actinin4 silencing increased motility in these cells (Figure 5). This observation is consistent with the role of alpha-actinin4 in actin cytoskeletal remodeling, and cells from alpha-actinin4 deficient mice exhibit increased motility [67]. Of note, injury leads to cytoskeleton remodeling and increased podocyte motility in culture and *in vivo* [68]. Accordingly, the decreased motility of PTP1B-deficient podocytes is in line with *in vivo* reports of PTP1B deficiency attenuating glomerular injury and protecting against proteinuria [32, 33] and hyperglycemia-induced renal injury [34]. Finally, the potential implications of PTP1B and alpha-actinin4 interactions on other aspects of podocyte function remain to be determined. In summary, previous and current findings suggest that targeting PTP1B and, plausibly, some of its substrates may present a therapeutic approach for podocyte injury and warrant additional investigation.

Funding:

Research in the Haj laboratory was funded by the National Institute of Diabetes and Digestive and Kidney Diseases grants R01DK095359 and R01DK090492, the National Institute of Environmental Health Sciences grant P42ES04699 and NIFA grant CA-D*-NTR-7836H. Additional support to the Haj laboratory for these studies includes funds from the Nora Eccles Treadwell Foundation. Dr. Hsu was supported in part by National Institute on Alcohol Abuse and Alcoholism grant R21AA027633. Research in the Meng laboratory is funded by the Academia Sinica Next-generation Pathway of Taiwan Cancer Precision Medicine Program Grant AS-KPQ-107-TCPMP. Research in the Wells laboratory is funded by grants from the National Institutes of Health (GM69688) and the Veterans Administration (Merit BX003368). The Olympus FV1000 confocal microscope located in the MCB Light Microscopy Imaging Facility (UC Davis Campus Core Research Facility) is supported by the National Institutes of Health Shared Instrumentation Grant 1S10RR019266-01.

References

1. Garg P (2018) A Review of Podocyte Biology. Am J Nephrol 47 Suppl 1:3–13 [PubMed: 29852492]
2. Fissell WH, Miner JH (2018) What Is the Glomerular Ultrafiltration Barrier? J Am Soc Nephrol 29:2262–2264 [PubMed: 30030419]
3. Cortes P, Mendez M, Riser BL, Guerin CJ, Rodriguez-Barbero A, Hassett C, Yee J (2000) F-actin fiber distribution in glomerular cells: structural and functional implications. Kidney Int 58:2452–2461 [PubMed: 11115078]
4. Kawachi H, Fukusumi Y (2020) New insight into podocyte slit diaphragm, a therapeutic target of proteinuria. Clin Exp Nephrol 24:193–204 [PubMed: 32020343]
5. Tian X, Ishibe S (2016) Targeting the podocyte cytoskeleton: from pathogenesis to therapy in proteinuric kidney disease. Nephrol Dial Transplant 31:1577–1583 [PubMed: 26968197]
6. Yu SM, Nissaisorakarn P, Husain I, Jim B (2018) Proteinuric Kidney Diseases: A Podocyte's Slit Diaphragm and Cytoskeleton Approach. Front Med (Lausanne) 5:221 [PubMed: 30255020]

7. Ylanne J, Scheffzek K, Young P, Saraste M (2001) Crystal structure of the alpha-actinin rod reveals an extensive torsional twist. Structure 9:597–604 [PubMed: 11470434]
8. Otey CA, Carpen O (2004) Alpha-actinin revisited: a fresh look at an old player. Cell Motil Cytoskeleton 58:104–111 [PubMed: 15083532]
9. Murphy AC, Young PW (2015) The actinin family of actin cross-linking proteins - a genetic perspective. Cell Biosci 5:49 [PubMed: 26312134]
10. Flood G, Kahana E, Gilmore AP, Rowe AJ, Gratzer WB, Critchley DR (1995) Association of structural repeats in the alpha-actinin rod domain. Alignment of inter-subunit interactions. J Mol Biol 252:227–234 [PubMed: 7674303]
11. Djinovic-Carugo K, Young P, Gautel M, Saraste M (1999) Structure of the alpha-actinin rod: molecular basis for cross-linking of actin filaments. Cell 98:537–546 [PubMed: 10481917]
12. Sjoblom B, Salmazo A, Djinovic-Carugo K (2008) Alpha-actinin structure and regulation. Cell Mol Life Sci 65:2688–2701 [PubMed: 18488141]
13. Goode NP, Shires M, Khan TN, Mooney AF (2004) Expression of alpha-actinin-4 in acquired human nephrotic syndrome: a quantitative immunoelectron microscopy study. Nephrol Dial Transplant 19:844–851 [PubMed: 15031339]
14. Feng D, Dumontier C, Pollak MR (2015) The role of alpha-actinin-4 in human kidney disease. Cell Biosci 5:44 [PubMed: 26301083]
15. Kaplan JM, Kim SH, North KN, Rennke H, Correia LA, Tong HQ, Mathis BJ, Rodriguez-Perez JC, Allen PG, Beggs AH, Pollak MR (2000) Mutations in ACTN4, encoding alpha-actinin-4, cause familial focal segmental glomerulosclerosis. Nat Genet 24:251–256 [PubMed: 10700177]
16. Weins A, Kenlan P, Herbert S, Le TC, Villegas I, Kaplan BS, Appel GB, Pollak MR (2005) Mutational and Biological Analysis of alpha-actinin-4 in focal segmental glomerulosclerosis. J Am Soc Nephrol 16:3694–3701 [PubMed: 16251236]
17. Michaud JL, Lemieux LI, Dube M, Vanderhyden BC, Robertson SJ, Kennedy CR (2003) Focal and segmental glomerulosclerosis in mice with podocyte-specific expression of mutant alpha-actinin-4. J Am Soc Nephrol 14:1200–1211 [PubMed: 12707390]
18. Henderson JM, Alexander MP, Pollak MR (2009) Patients with ACTN4 mutations demonstrate distinctive features of glomerular injury. J Am Soc Nephrol 20:961–968 [PubMed: 19357256]
19. Kanchanawong P, Shtengel G, Pasapera AM, Ramko EB, Davidson MW, Hess HF, Waterman CM (2010) Nanoscale architecture of integrin-based cell adhesions. Nature 468:580–584 [PubMed: 21107430]
20. Shao H, Wang JH, Pollak MR, Wells A (2010) alpha-actinin-4 is essential for maintaining the spreading, motility and contractility of fibroblasts. PLoS One 5:e13921 [PubMed: 21085685]
21. Cybulsky AV, Kennedy CR (2011) Podocyte Injury Associated with Mutant alpha-Actinin-4. J Signal Transduct 2011:563128 [PubMed: 21808733]
22. Shao H, Wingert B, Weins A, Pollak MR, Camacho C, Wells A (2019) Focal segmental glomerulosclerosis ACTN4 mutants binding to actin: regulation by phosphomimetic mutations. Sci Rep 9:15517 [PubMed: 31664084]
23. Shao H, Wu C, Wells A (2010) Phosphorylation of alpha-actinin 4 upon epidermal growth factor exposure regulates its interaction with actin. J Biol Chem 285:2591–2600 [PubMed: 19920151]
24. Shao H, Wells A (2021) Binding of alpha-ACTN4 to EGF receptor enables its rapid phosphorylation. Heliyon 7:e06011 [PubMed: 33532643]
25. Feng Y, Ngu H, Alford SK, Ward M, Yin F, Longmore GD (2013) alpha-actinin1 and 4 tyrosine phosphorylation is critical for stress fiber establishment, maintenance and focal adhesion maturation. Exp Cell Res 319:1124–1135 [PubMed: 23454549]
26. Frangioni JV, Beahm PH, Shifrin V, Jost CA, Neel BG (1992) The nontransmembrane tyrosine phosphatase PTP-1B localizes to the endoplasmic reticulum via its 35 amino acid C-terminal sequence. Cell 68:545–560 [PubMed: 1739967]
27. Haj FG, Verveer PJ, Squire A, Neel BG, Bastiaens PI (2002) Imaging sites of receptor dephosphorylation by PTP1B on the surface of the endoplasmic reticulum. Science 295:1708–1711 [PubMed: 11872838]
28. Tonks NK (2003) PTP1B: From the sidelines to the front lines! FEBS Lett 546:140–148 [PubMed: 12829250]

29. Bakke J, Haj FG (2015) Protein-tyrosine phosphatase 1B substrates and metabolic regulation. Semin Cell Dev Biol 37C:58–65
30. Yip SC, Saha S, Chernoff J (2010) PTP1B: a double agent in metabolism and oncogenesis. Trends Biochem Sci 35:442–449 [PubMed: 20381358]
31. Feldhammer M, Uetani N, Miranda-Saavedra D, Tremblay ML (2013) PTP1B: a simple enzyme for a complex world. Crit Rev Biochem Mol Biol 48:430–445 [PubMed: 23879520]
32. Nezvitsky L, Tremblay ML, Takano T, Papillon J, Cybulsky AV (2014) Complement-mediated glomerular injury is reduced by inhibition of protein-tyrosine phosphatase 1B. Am J Physiol Renal Physiol 307:F634–647 [PubMed: 25056348]
33. Kumagai T, Baldwin C, Aoudjit L, Nezvitsky L, Robins R, Jiang R, Takano T (2014) Protein tyrosine phosphatase 1B inhibition protects against podocyte injury and proteinuria. Am J Pathol 184:2211–2224 [PubMed: 24951831]
34. Ito Y, Hsu MF, Bettaieb A, Koike S, Mello A, Calvo-Rubio M, Villalba JM, Haj FG (2017) Protein tyrosine phosphatase 1B deficiency in podocytes mitigates hyperglycemia-induced renal injury. Metabolism 76:56–69 [PubMed: 28987240]
35. Aoudjit L, Jiang R, Lee TH, New LA, Jones N, Takano T (2011) Podocyte Protein, Nephrin, Is a Substrate of Protein Tyrosine Phosphatase 1B. J Signal Transduct 2011:376543 [PubMed: 22013520]
36. Welsh GI, Hale LJ, Eremina V, Jeansson M, Maezawa Y, Lennon R, Pons DA, Owen RJ, Satchell SC, Miles MJ, Caunt CJ, Mcardle CA, Pavenstadt H, Tavare JM, Herzenberg AM, Kahn CR, Mathieson PW, Quaggin SE, Saleem MA, Coward RJ (2010) Insulin signaling to the glomerular podocyte is critical for normal kidney function. Cell Metab 12:329–340 [PubMed: 20889126]
37. Saito T, Yamada E, Okada S, Shimoda Y, Tagaya Y, Hashimoto K, Satoh T, Mori M, Okada J, Pessin JE, Yamada M (2014) Nucleobindin-2 is a positive regulator for insulin-stimulated glucose transporter 4 translocation in fenofibrate treated E11 podocytes. Endocr J 61:933–939 [PubMed: 25168660]
38. Bettaieb A, Liu S, Xi Y, Nagata N, Matsuo K, Matsuo I, Chahed S, Bakke J, Keilhack H, Tiganis T, Haj FG (2011) Differential regulation of endoplasmic reticulum stress by protein tyrosine phosphatase 1B and T cell protein tyrosine phosphatase. J Biol Chem 286:9225–9235 [PubMed: 21216966]
39. Bakke J, Bettaieb A, Nagata N, Matsuo K, Haj FG (2013) Regulation of the SNARE-interacting protein Munc18c tyrosine phosphorylation in adipocytes by protein-tyrosine phosphatase 1B. Cell Commun Signal 11:57 [PubMed: 23937695]
40. Matsuo K, Bettaieb A, Nagata N, Matsuo I, Keilhack H, Haj FG (2011) Regulation of brown fat adipogenesis by protein tyrosine phosphatase 1B. PLoS One 6:e16446 [PubMed: 21305007]
41. Kelly AD, Breitkopf SB, Yuan M, Goldsmith J, Spentzos D, Asara JM (2011) Metabolomic profiling from formalin-fixed, paraffin-embedded tumor tissue using targeted LC/MS/MS: application in sarcoma. PLoS One 6:e25357 [PubMed: 21984915]
42. Bence KK, Delibegovic M, Xue B, Gorgun CZ, Hotamisligil GS, Neel BG, Kahn BB (2006) Neuronal PTP1B regulates body weight, adiposity and leptin action. Nat Med 12:917–924 [PubMed: 16845389]
43. Flint AJ, Tiganis T, Barford D, Tonks NK (1997) Development of “substrate-trapping” mutants to identify physiological substrates of protein tyrosine phosphatases. Proc Natl Acad Sci U S A 94:1680–1685 [PubMed: 9050838]
44. Andersen JN, Mortensen OH, Peters GH, Drake PG, Iversen LF, Olsen OH, Jansen PG, Andersen HS, Tonks NK, Moller NP (2001) Structural and evolutionary relationships among protein tyrosine phosphatase domains. Mol Cell Biol 21:7117–7136 [PubMed: 11585896]
45. Stuible M, Dube N, Tremblay ML (2008) PTP1B regulates cortactin tyrosine phosphorylation by targeting Tyr446. J Biol Chem 283:15740–15746 [PubMed: 18387954]
46. Salmeen A, Andersen JN, Myers MP, Tonks NK, Barford D (2000) Molecular basis for the dephosphorylation of the activation segment of the insulin receptor by protein tyrosine phosphatase 1B. Mol Cell 6:1401–1412 [PubMed: 11163213]
47. Rikova K, Guo A, Zeng Q, Possemato A, Yu J, Haack H, Nardone J, Lee K, Reeves C, Li Y, Hu Y, Tan Z, Stokes M, Sullivan L, Mitchell J, Wetzel R, Macneill J, Ren JM, Yuan J, Bakalarski CE,

Villen J, Kornhauser JM, Smith B, Li D, Zhou X, Gygi SP, Gu TL, Polakiewicz RD, Rush J, Comb MJ (2007) Global survey of phosphotyrosine signaling identifies oncogenic kinases in lung cancer. Cell 131:1190–1203 [PubMed: 18083107]

48. Mertins P, Eberl HC, Renkawitz J, Olsen JV, Tremblay ML, Mann M, Ullrich A, Daub H (2008) Investigation of protein-tyrosine phosphatase 1B function by quantitative proteomics. Mol Cell Proteomics 7:1763–1777 [PubMed: 18515860]
49. Bettaieb A, Matsuo K, Matsuo I, Wang S, Melhem R, Koromilas AE, Haj FG (2012) Protein tyrosine phosphatase 1B deficiency potentiates PERK/eIF2alpha signaling in brown adipocytes. PLoS One 7:e34412 [PubMed: 22509299]
50. Bettaieb A, Bakke J, Nagata N, Matsuo K, Xi Y, Liu S, Aboubechara D, Melhem R, Stanhope K, Cummings B, Graham J, Bremer A, Zhang S, Lyssiotis CA, Zhang ZY, Cantley LC, Havel PJ, Haj FG (2013) Protein tyrosine phosphatase 1B regulates pyruvate kinase M2 tyrosine phosphorylation. J Biol Chem 288:17360–17371 [PubMed: 23640882]
51. Liu S, Xi Y, Bettaieb A, Matsuo K, Matsuo I, Kulkarni RN, Haj FG (2014) Disruption of protein-tyrosine phosphatase 1B expression in the pancreas affects beta-cell function. Endocrinology 155:3329–3338 [PubMed: 24956127]
52. Kimura M, Toyoda M, Kato M, Kobayashi K, Abe M, Kobayashi T, Miyauchi M, Yamamoto N, Umezono T, Suzuki D (2008) Expression of alpha-actinin-4 in human diabetic nephropathy. Intern Med 47:1099–1106 [PubMed: 18552466]
53. Haj FG, Markova B, Klaman LD, Bohmer FD, Neel BG (2003) Regulation of receptor tyrosine kinase signaling by protein tyrosine phosphatase-1B. J Biol Chem 278:739–744 [PubMed: 12424235]
54. Bjorge JD, Pang A, Fujita DJ (2000) Identification of protein-tyrosine phosphatase 1B as the major tyrosine phosphatase activity capable of dephosphorylating and activating c-Src in several human breast cancer cell lines. J Biol Chem 275:41439–41446 [PubMed: 11007774]
55. Huyer G, Liu S, Kelly J, Moffat J, Payette P, Kennedy B, Tsaprailis G, Gresser MJ, Ramachandran C (1997) Mechanism of inhibition of protein-tyrosine phosphatases by vanadate and pervanadate. J Biol Chem 272:843–851 [PubMed: 8995372]
56. Travers T, Shao H, Joughin BA, Lauffenburger DA, Wells A, Camacho CJ (2015) Tandem phosphorylation within an intrinsically disordered region regulates ACTN4 function. Sci Signal 8:ra51 [PubMed: 26012634]
57. Zhang Z, Lin SY, Neel BG, Haimovich B (2006) Phosphorylated alpha-actinin and protein-tyrosine phosphatase 1B coregulate the disassembly of the focal adhesion kinase x Src complex and promote cell migration. J Biol Chem 281:1746–1754 [PubMed: 16291744]
58. Myers MP, Andersen JN, Cheng A, Tremblay ML, Horvath CM, Parisien JP, Salmeen A, Barford D, Tonks NK (2001) TYK2 and JAK2 are substrates of protein-tyrosine phosphatase 1B. J Biol Chem 276:47771–47774 [PubMed: 11694501]
59. Uchida K, Suzuki K, Iwamoto M, Kawachi H, Ohno M, Horita S, Nitta K (2008) Decreased tyrosine phosphorylation of nephrin in rat and human nephrosis. Kidney Int 73:926–932 [PubMed: 18256598]
60. Denhez B, Lizotte F, Guimond MO, Jones N, Takano T, Geraldes P (2015) Increased SHP-1 protein expression by high glucose levels reduces nephrin phosphorylation in podocytes. J Biol Chem 290:350–358 [PubMed: 25404734]
61. Verma R, Venkatareddy M, Kalinowski A, Patel SR, Salant DJ, Garg P (2015) Shp2 Associates with and Enhances Nephrin Tyrosine Phosphorylation and Is Necessary for Foot Process Spreading in Mouse Models of Podocyte Injury. Mol Cell Biol 36:596–614 [PubMed: 26644409]
62. Hsu MF, Bettaieb A, Ito Y, Graham J, Havel PJ, Haj FG (2017) Protein tyrosine phosphatase Shp2 deficiency in podocytes attenuates lipopolysaccharide-induced proteinuria. Sci Rep 7:461 [PubMed: 28352079]
63. Haj FG, Sabet O, Kinkhabwala A, Wimmer-Kleikamp S, Roukos V, Han HM, Grabenbauer M, Bierbaum M, Antony C, Neel BG, Bastiaens PI (2012) Regulation of signaling at regions of cell-cell contact by endoplasmic reticulum-bound protein-tyrosine phosphatase 1B. PLoS One 7:e36633 [PubMed: 22655028]

64. Chakraborty S, Reineke EL, Lam M, Li X, Liu Y, Gao C, Khurana S, Kao HY (2006) Alpha-actinin 4 potentiates myocyte enhancer factor-2 transcription activity by antagonizing histone deacetylase 7. J Biol Chem 281:35070–35080 [PubMed: 16980305]

65. Khurana S, Chakraborty S, Zhao X, Liu Y, Guan D, Lam M, Huang W, Yang S, Kao HY (2012) Identification of a novel LXXLL motif in alpha-actinin 4-spliced isoform that is critical for its interaction with estrogen receptor alpha and co-activators. J Biol Chem 287:35418–35429 [PubMed: 22908231]

66. Zhao X, Hsu KS, Lim JH, Bruggeman LA, Kao HY (2015) alpha-Actinin 4 potentiates nuclear factor kappa-light-chain-enhancer of activated B-cell (NF-kappaB) activity in podocytes independent of its cytoplasmic actin binding function. J Biol Chem 290:338–349 [PubMed: 25411248]

67. Kos CH, Le TC, Sinha S, Henderson JM, Kim SH, Sugimoto H, Kalluri R, Gerszten RE, Pollak MR (2003) Mice deficient in alpha-actinin-4 have severe glomerular disease. J Clin Invest 111:1683–1690 [PubMed: 12782671]

68. Brahler S, Yu H, Suleiman H, Krishnan GM, Saunders BT, Kopp JB, Miner JH, Zinselmeyer BH, Shaw AS (2016) Intravital and Kidney Slice Imaging of Podocyte Membrane Dynamics. J Am Soc Nephrol 27:3285–3290 [PubMed: 27036737]

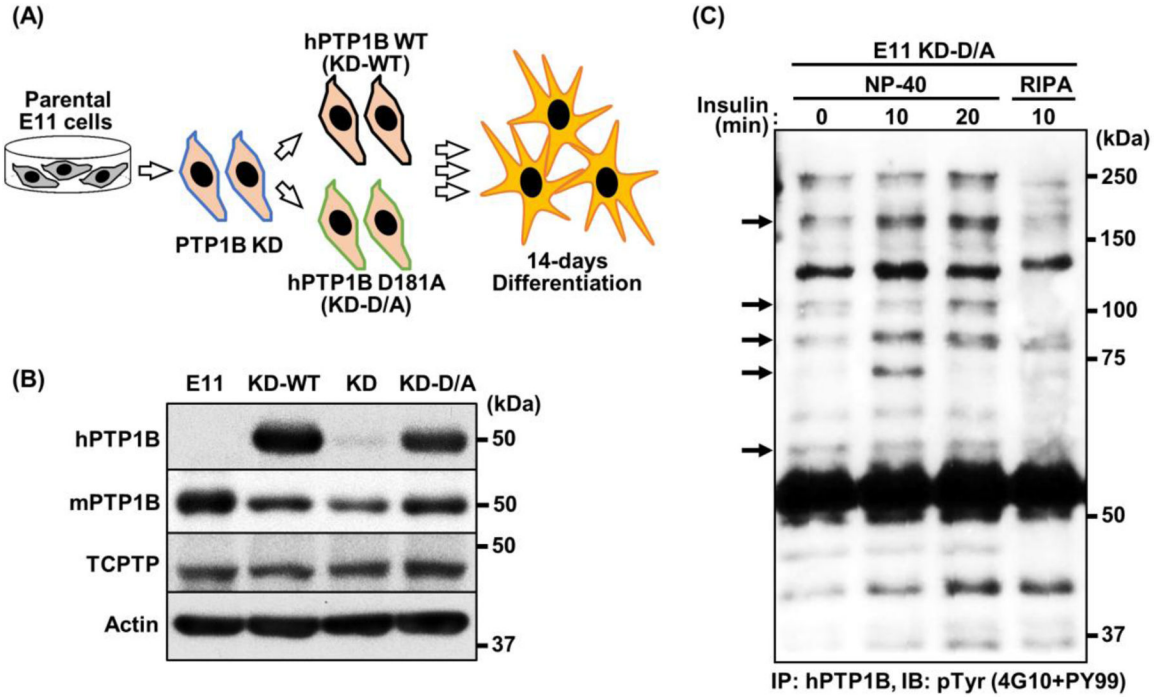

(D)

Ranking	Protein name	Accession number	Predicted MW (KDa)	YY motif
1	Src substrate cortactin	Q60598	61	-
2	LIM domain and actin-binding protein 1	Q9ERG0	84	$RY^{745}Y^{746}D$
3	Alpha-actinin-4	P57780	105	$DY^{486}Y^{487}D$
4	Heat shock cognate 71 kDa protein	P63017	71	-
5	ATP-dependent RNA helicase	Q62167	73	-

Figure 1: Identification of putative PTP1B substrates in podocytes.

(A) E11 murine kidney podocyte cell line with PTP1B knockdown (KD) was reconstituted with shRNA-resistant hPTP1B wild-type (KD-WT) and substrate-trapping hPTP1B D181A (KD-D/A) mutant. Cells were grown at 33°C until confluency and then differentiated into podocytes by the culture at 37°C for 14 days, as indicated in the schematic. **(B)** Immunoblots of hPTP1B (FG6), mPTP1B, and TCPTP in the parental E11 cell line and cells with PTP1B knockdown (KD) and reconstitution (KD-WT and KD-D/A). Blots were probed with Actin as a loading control. **(C)** 14 days-differentiated KD-D/A podocytes were serum starved overnight and stimulated with insulin for the indicated times, then lysed in NP-40 or RIPA buffer. hPTP1B was immunoprecipitated (IP) from KD-D/A podocytes, then immunoblotted for phospho-tyrosine (pTyr; 4G10 and PY99). Bands corresponding to hyper-phosphorylated proteins are indicated by arrows. A comparable gel was stained with Instant Blue solution, and bands that included the hyper-phosphorylated proteins were excised and subjected to mass spectroscopy. The MS analysis was performed once

to identify the putative substrates. **(D)** List of top five putative PTP1B substrates (name, accession number, predicted molecular weight, and bis-phosphorylated motif) listed by identification hits in the screen.

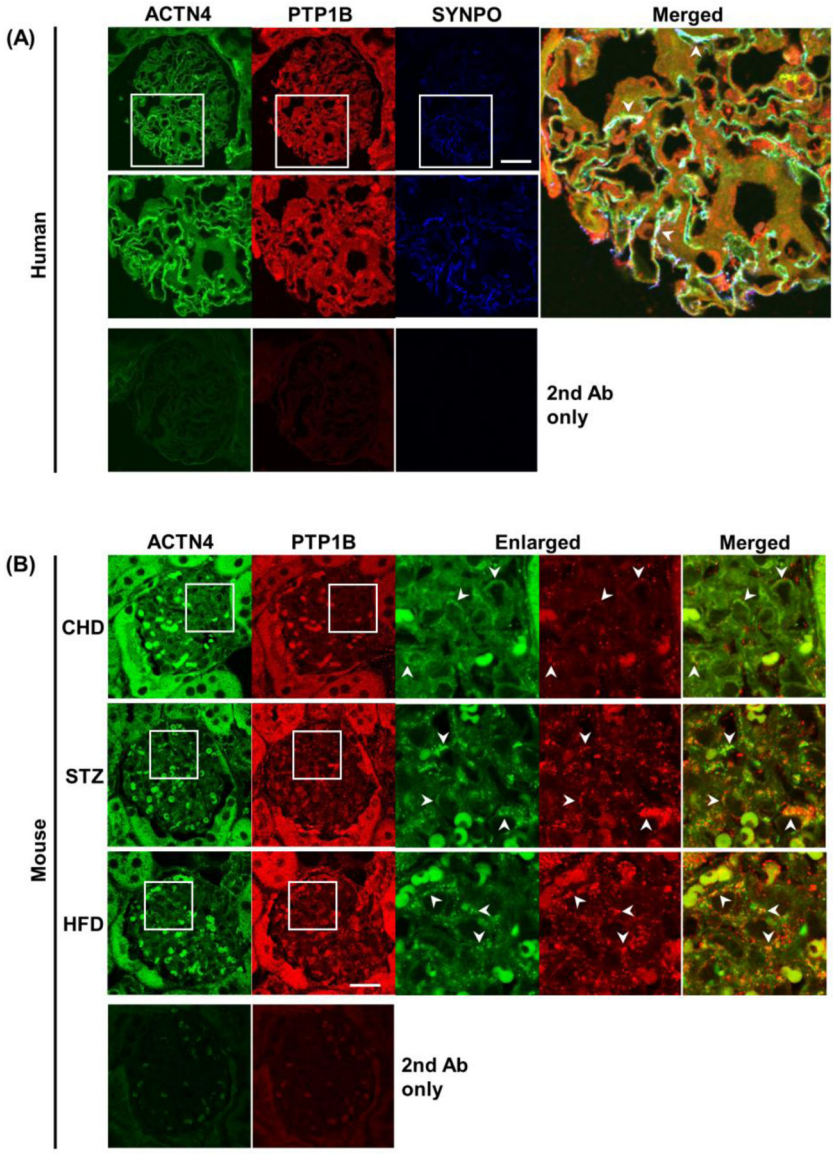

Figure 2: Co-localization of endogenous alpha-actinin4 and PTP1B in human and murine glomeruli.

(A) Immunostaining and confocal microscopy of ACTN4 (green), PTP1B (red), and podocyte marker Synaptopodin (SYNPO) in the kidney section of a human control subject. Images in the lower panel are a magnification of the boxed region, and a merged picture was enlarged on the right. Scale bar: 50μm. **(B)** Immunostaining and confocal microscopy of ACTN4 (green) and PTP1B (red) in kidney sections of male mice fed standard laboratory chow (CHD), streptozotocin (STZ; 13 weeks)-treated and fed a high-fat diet (HFD; 25 weeks). Enlarged and merged images in the right panel are the zoom-in views of the boxed regions. Representative images were shown from two mice per group. Scale bar: 20μm. The sample incubated with only the secondary antibodies (2nd Ab only) served as background control. Co-localization is indicated by an arrowhead.

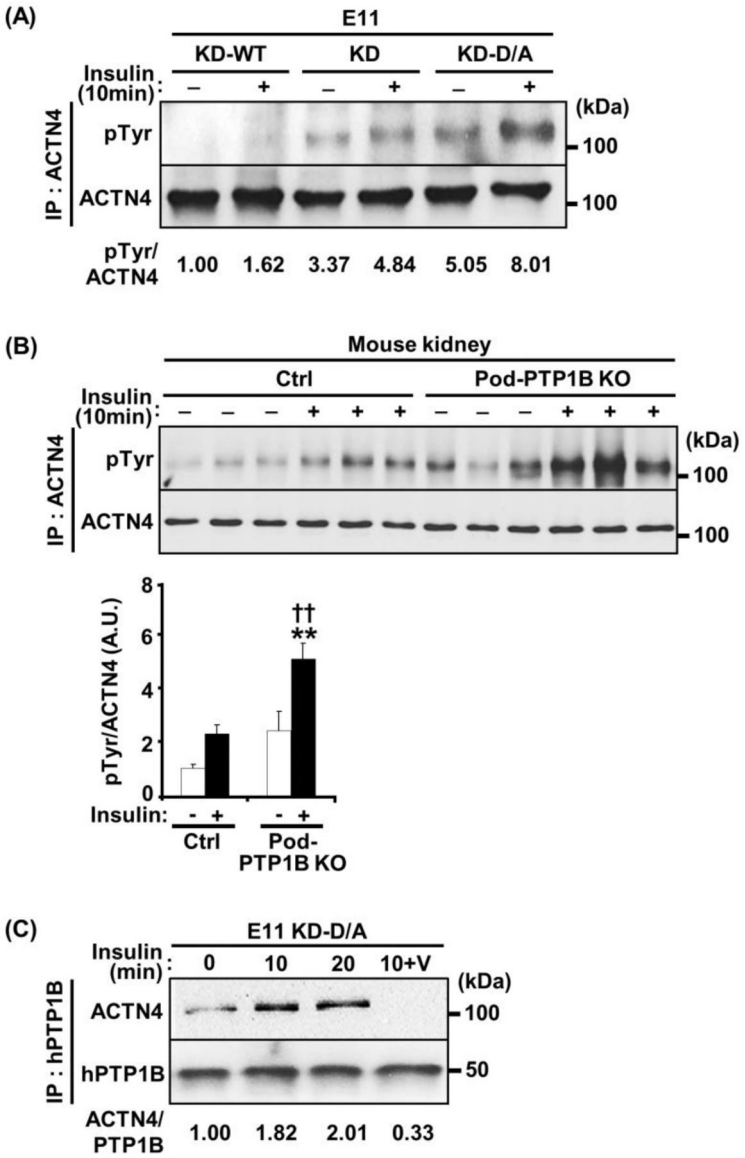

Figure 3: Interaction of PTP1B and alpha-actinin4.

(A) ACTN4 was immunoprecipitated (IP) from 14 days-differentiated E11 cells with knockdown (KD) and reconstituted expression of PTP1B (KD-WT and KD-D/A) under basal (−) and insulin-stimulation (+) for 10 minutes, then immunoblotted for phospho-tyrosine (pTyr) and ACTN4. The blot images were obtained from one attempt experiment and quantified as a relative ratio of pTyr/ACTN4. **(B)** ACTN4 was immunoprecipitated from kidney lysates of control (Ctrl; *Ptpn1*$^{fl/fl}$) and podocyte PTP1B knockout (pod-PTP1B KO; *Ptpn1*$^{fl/fl}$ Pod-cre^{+}) mice under basal (−) and insulin-stimulation (+, 10 min), then immunoblotted for pTyr and ACTN4. Each lane represents lysate from a different animal, and the blot images were quantified and presented in a bar chart (n=3/group). $^{**}p \leq 0.01$ indicate a significant difference between without versus with insulin of the pod-PTP1B KO mice; $\dagger\dagger p \leq 0.01$ indicates a significant difference between Ctrl versus pod-PTP1B KO mice with insulin. **(C)** 14 days-differentiated PTP1B KD-D/A podocytes were serum starved

overnight, then stimulated with insulin for the indicated times, and lysed in NP-40 without and with vanadate (V) treatment. hPTP1B was immunoprecipitated and then immunoblotted for ACTN4 and hPTP1B. The blot images were obtained from one attempt experiment and quantified in relative ratio as ACTN4/PTP1B.

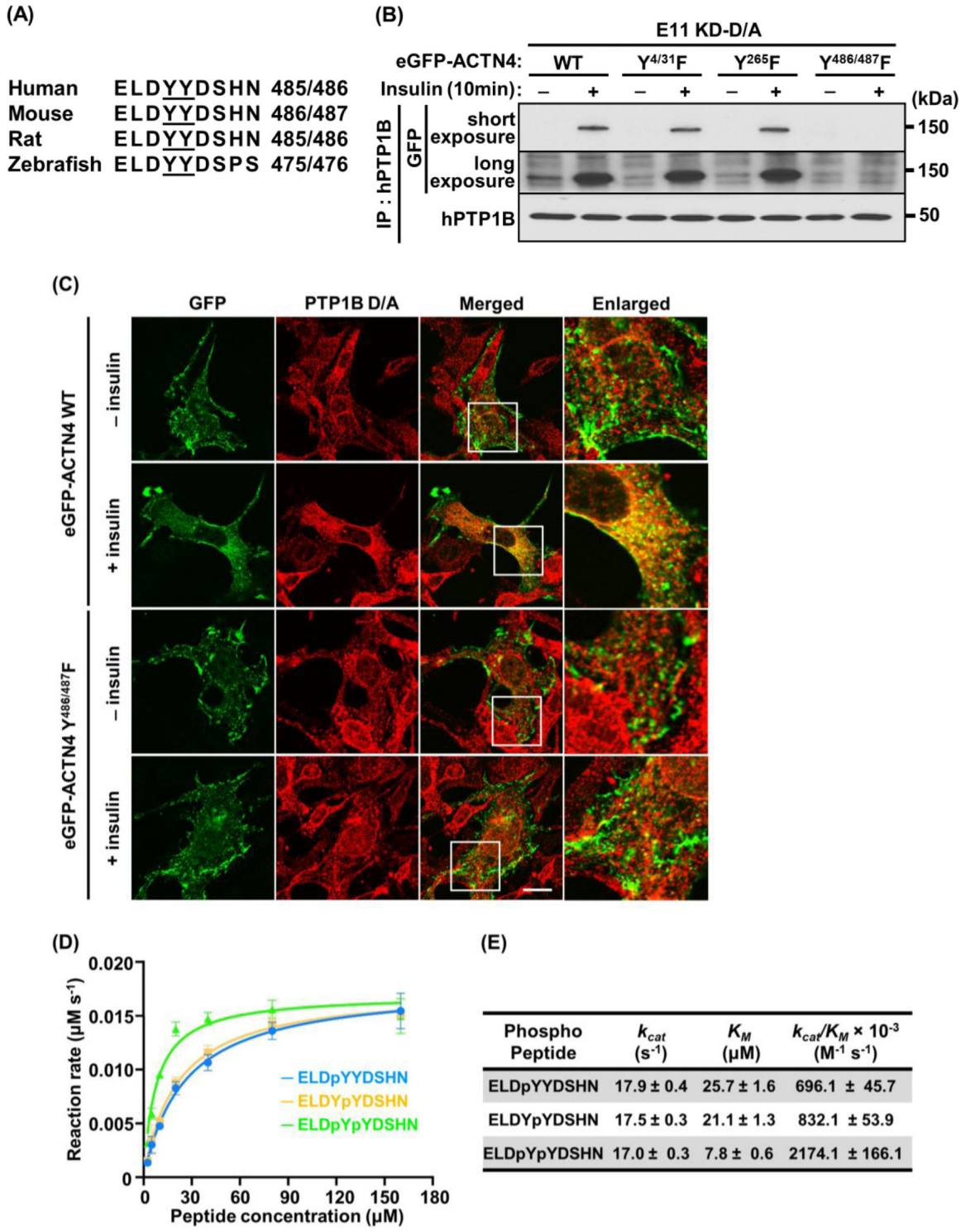

Phospho Peptide	k_{cat} (s^{-1})	K_M (μM)	$k_{cat}/K_M \times 10^{-3}$ ($M^{-1}\ s^{-1}$)
ELDpYYDSHN	17.9 ± 0.4	25.7 ± 1.6	696.1 ± 45.7
ELDYpYDSHN	17.5 ± 0.3	21.1 ± 1.3	832.1 ± 53.9
ELDpYpYDSHN	17.0 ± 0.3	7.8 ± 0.6	2174.1 ± 166.1

Figure 4: The alpha-actinin4 tandem tyrosine-phosphorylated motif mediates the interaction with PTP1B.

(A) Aligned sequences across species relative to $Tyr^{486/487}$ (underlined) of mouse ACTN4.

(B) PTP1B KD-D/A E11 cells were transfected with eGFP-ACTN4 WT and Y/F mutants ($Y^{4/31}F$, $Y^{265}F$, and $Y^{486/487}F$). hPTP1B was immunoprecipitated (IP) from serum starved

(−) and insulin-stimulated (+, 10 min) cells, then immunoblotted using antibodies for GFP and PTP1B. The middle blot for GFP depicts a longer exposure time of the same membrane in the top blot. The blot images were obtained from one attempt experiment. **(C)** Immunofluorescence of KD-D/A E11 cells transfected with eGFP-ACTN4 WT and $Y^{486/487}F$ under basal (-, serum starved) and insulin-stimulated (+, 10 min) states. hPTP1B (red) and ACTN4 (green) were detected using FG6 and GFP antibodies, respectively. Enlarged images are highlighted by white boxes in the merged panel. Scale bar: 5μm. Representative images were shown from two independent experiments. **(D)** Michaelis-Menten curves showing dephosphorylation of mono- and di-phospho tyrosine peptides derived from alpha-actinin4 by purified PTP1B (n=9). **(E)** Summary of kinetic parameters determined by Michaelis-Menten equation.

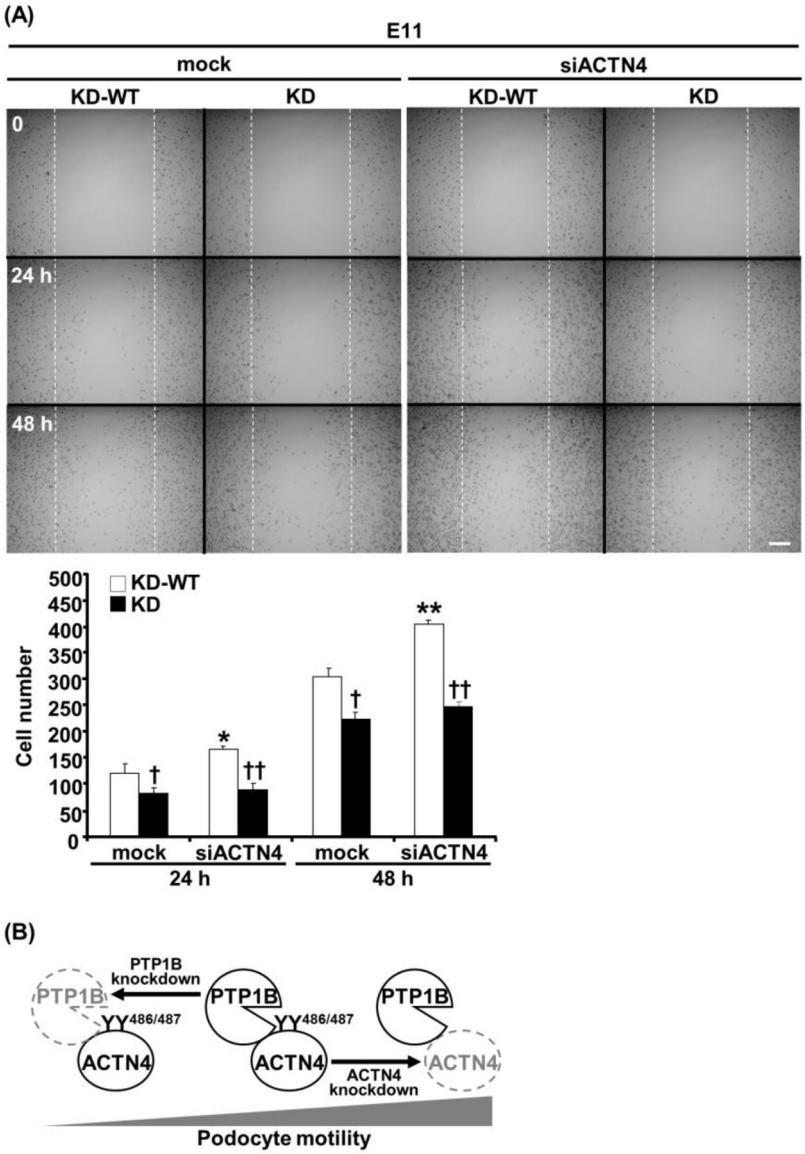

Figure 5: Alpha-actinin4 silencing increases motility in podocytes.

(A) Images of bright-field microscopy and quantification of cell numbers in the wound areas of PTP1B KD-WT and KD E11 cells without and with siRNA-mediated silencing of ACTN4 at 24 and 48 hours post 10% FBS stimulation (n=3/group). Scale bar: 100μm. *$p \leq 0.05$ and **$p \leq 0.01$ indicate a significant difference between mock versus siACTN4 of the same cell type at either 24h or 48h; †$p \leq 0.05$, ††$p \leq 0.01$ indicates a significant difference between KD-WT versus KD cells with the same treatment at either 24h or 48h. **(B)** Schematic representation of the interaction of PTP1B and ACTN4 in regulating podocyte motility.